Thermal modelling for the implementation of an energetic efficiency control system in a room of meetings of singular geometry

Vicente Fuster[*,1], José Fernández B[1], Manuel J. Martínez B.[1], Ignacio Benítez S[1].
[1]Instituto Tecnológico de la Energía (ITE), Paterna, Valencia, Spain.
*Corresponding author: laboratorios@ite.es

Abstract: The aim of this Project is to obtain a temporary and spatial evolution model of the temperature into a meeting room with the aim to develop an efficient energy mechanism which can improve the air conditioner control system. To optimize the air conditioning control system and promote energy efficiency we must know the evolution of the irradiance along the day and depending on the season of the year. The project has considered two extremes cases: on the one hand a typical summer day and on the other hand a winter day. From annual data of the Institute weather station a representative irradiance values have been obtained: an average of June and July months for summer and an average of December and January months for winter. To analyze the air conditioning control system improvement the Finite Element technique has been used by means the Comsol tool.

Keywords: irradiance, Finite Element technique, numerical analysis, modeling and simulation.

1 Introduction

The aim of this work is to model the heat load in rooms, in this case, a meeting room whose shape is shown in Figure 1 in order to study the energetic savings that can produce an automatic control system applied to this place maintaining the comfort level of its occupants.

The modeling of the heat loads of the enclosure can delimit the temperature conditions of comfort [1] according a number of variables among which can include: irradiance, ambient temperature, intensity and temperature of air conditioning, number of persons present on site, time of day, month, among others.

Given the geometry of the enclosure and the materials used in its construction, external walls of glass, the main variable will exercise great influence in thermal loads modeling is the irradiance.

To do this, the irradiance data provided by the meteorological station of the Institute are corrected due to the orientation of the faces of the façade. Below the polynomial functions that match the values provided are determined. Then, through the tool Comsol, the problem is raised by means the Finite Element method.

The Finite Element method emerged on the idea of Hrenicoff [2] who suggested the idea that, under certain restrictions on loading, the elastic behavior of a continuous slab could resemble a set of elements connected together by means of discrete points. As the use of computers was intensified the matrix theory was adapted to the use of this equipment. In this way, Turner, Clough, Martin and Topp [2] assembling pieces of triangular shape in the modeling of aircraft structures and relating them to a matrix structural analysis, produced a systematic procedure similar to what later became known as Finite Elements. Because of the way in which the finite element method has been adapted to the computing capabilities, the use of this method has been growing rapidly through the years. Special mention deserves Zienkiewicz's [3] contributions who, in addition to the application of the finite element method to the structural problems, adapted the finite element theory to the field problems that were using the Laplace or Poisson equations such as heat conduction problems in steady state and potential flow of an incompressible fluid.

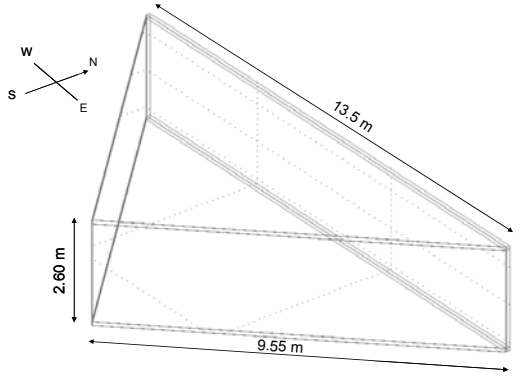

Figure 1 Enclosure scheme.

2 Development

At this stage the appropriate boundary conditions are defined and the polynomial expressions of irradiance for each external face are introduced. Finally an evolution model of the room temperature is obtained over a day of summer or winter. These results are compared with experimental data obtained in the enclosure to ensure the suitability of the model.

The analysis room has an area of 45.56 m^2, a height of 2.6 m and a volume of 118.46 m^3, see Figure 1. The modeling takes into account the incident irradiance for each external face, which varies depending on the time of day. Global irradiance data was obtained from the meteorological station of the Institute. The summer irradiance has been calculated based on an average of 20 days, from June 20 to June 27 and from July 5 to July 15. For the winter has been taken into consideration the average of 15 days from December 26 to January 15. Table 1 shows the levels of incident irradiance for every seasonal period. Because throughout the day both areas receive different heat inputs depending on the orientation (from a reference point on the planet), the incident irradiance on each surface should be adjusted by means of the calculation of incident coefficients. From statistical data of PVGIS [4] the coefficients obtained are shown in Table 2 and Table 3. Figure 2 and Figure 3 show the curves of the surfaces irradiance at each seasonal period. Winter irradiance assumes clear skies.

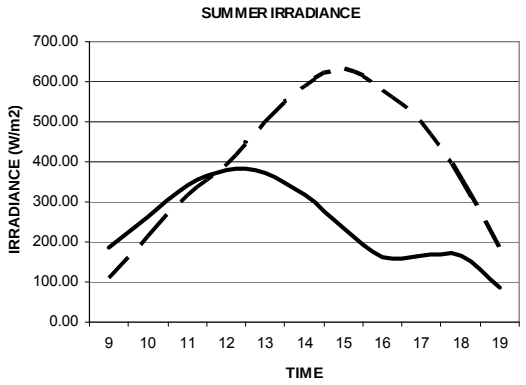

Figure 2 Irradiance curve for summer. Averaged curves for every face. ——, east face; – – –, west face.

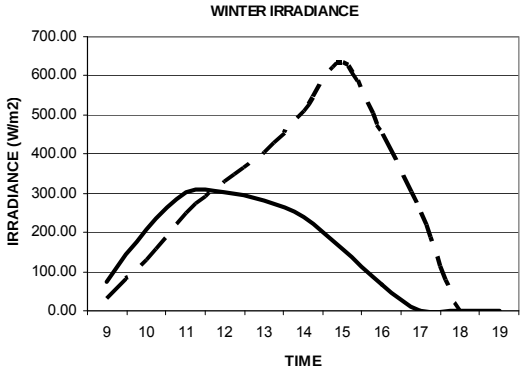

Figure 3 Irradiance curve for winter. Averaged curves for every face. ——, east face; – – –, west face.

2.1 Simulation scenarios

The triangular shaped room modeling provides a variety of scenarios based on the following parameters:

- Time of day. There are three divisions: morning (9 to 12), noon (12 to 16) and later (16 to 19).
- Weather station: summer or winter.
- Existence or not of air conditioning.
- Number of persons. It will be analyzed the cases in which the room is empty and a usual number of people are gathered (from five to ten).

In order to validate the Finite Element model, measures of the temperature at five different points have been made.

2.2 Fitting curves

After adjusting the irradiance data is necessary to obtain the mathematical model, fitted to the initial data, in order to be introduced in the tool Comsol. The mathematical models are polynomial curves that, given the characteristics of the irradiance data, are odd curves. From the data shown in Table 2 for the summer:

east face:

$$Irrad_{ver,E} = 5.74\cdot10^{-5}x^9 - 2.11\cdot10^{-3}x^8 + 0.027x^7 - 0.13x^6 - 0.0894x^5 + 2.8178x^4 - 11.4836x^3 + 19.675x^2 + 68.0458x + 106.835 \quad (1)$$

west face:

$$Irrad_{ver,O} = 2.467\cdot10^{-4}x^9 - 0.0115x^8 + 0.219x^7 - 2.146x^6 + 11.227x^5 - 28.553x^4 + 18.761x^3 + 44.859x^2 + 38.910x + 23.081 \quad (2)$$

For the winter the data shown in Table 3 indicates:

east face:

$$Irrad_{inv,E} = 1.598\cdot10^{-4}x^9 - 0.008x^8 + 0.177x^7 - 1.965x^6 + 11.912x^5 - 36.571x^4 + 33.981x^3 + 54.017x^2 + 23.841x - 14.832 \quad (3)$$

west face:

$$Irrad_{inv,O} = -6.39\cdot10^{-5}x^9 + 8.99\cdot10^{-4}x^8 + 0.026x^7 - 0.762x^6 + 6.463x^5 - 24.772x^4 + 30.239x^3 + 37.999x^2 - 5.974x - 30.031 \quad (4)$$

Figure 4 and Figure 5 show the curves of the recorded data and the polynomial fit.

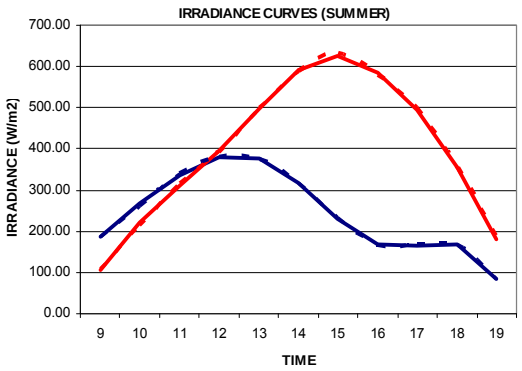

Figure 4 Irradiance curve fitting (Summer).
East face: ——, fitted; – – –, recorded.
West face: ——, fitted; – – –, recorded.

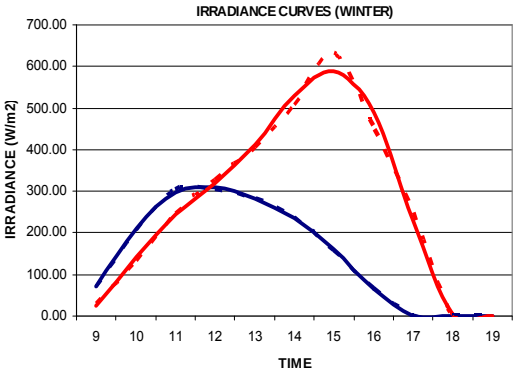

Figure 5 Irradiance curve fitting (Winter).
East face: ——, fitted; – – –, recorded.
West face: ——, fitted; – – –, recorded.

The results show a good fit of polynomial functions with the recorded data.

3 Use of COMSOL Multiphysics

This section describes the problem approach to be solved through numerical techniques such as the Finite Element method, through the tool Comsol. The analysis approach involves:

- Consideration of forced entry of air, hot or cold.
- Enclosure isolation.
- The properties of air are constants with reference to the atmospheric temperature.
- Air enters through the inlet.
- External walls are made of glass (cathetus of the triangle).

Based on these assumptions the equations governing the behavior of the system are [5, 6]:

$$\frac{\partial\rho}{\partial t} + \frac{\partial(\rho u)}{\partial x} + \frac{\partial(\rho v)}{\partial y} + \frac{\partial(\rho w)}{\partial z} \quad (5)$$

$$\rho a_x = \rho F_x - \frac{\partial p}{\partial x} + \frac{\partial}{\partial x}\left(2\mu\frac{\partial u}{\partial x} + \left(\zeta - \frac{2}{3}\mu\right)\nabla^T \vec{u}\right) + \frac{\partial}{\partial y}\left(\mu\left(\frac{\partial u}{\partial y} + \frac{\partial v}{\partial x}\right)\right) + \frac{\partial}{\partial z}\left(\mu\left(\frac{\partial u}{\partial z} + \frac{\partial w}{\partial x}\right)\right) \quad (6)$$

$$\rho a_y = \rho F_y - \frac{\partial p}{\partial y} + \frac{\partial}{\partial y}\left(2\mu\frac{\partial v}{\partial y} + \left(\zeta - \frac{2}{3}\mu\right)\nabla^T \vec{u}\right) + \frac{\partial}{\partial z}\left(\mu\left(\frac{\partial v}{\partial z} + \frac{\partial w}{\partial y}\right)\right) + \frac{\partial}{\partial x}\left(\mu\left(\frac{\partial v}{\partial x} + \frac{\partial u}{\partial y}\right)\right) \quad (7)$$

$$\rho a_z = \rho F_z - \frac{\partial p}{\partial z} + \frac{\partial}{\partial z}\left(2\mu\frac{\partial w}{\partial z} + \left(\zeta - \frac{2}{3}\mu\right)\nabla^T \vec{u}\right) + \frac{\partial}{\partial x}\left(\mu\left(\frac{\partial w}{\partial x} + \frac{\partial u}{\partial z}\right)\right) + \frac{\partial}{\partial y}\left(\mu\left(\frac{\partial w}{\partial y} + \frac{\partial v}{\partial z}\right)\right) \quad (8)$$

where u, v, and w are the components of the velocity in the x, y and z axes, ρ is the density, t the time, F_x, F_y, F_z the volumetric forces, p the pressure, μ is the dynamic viscosity and ζ is the second viscosity term, where its value is 0 for monatomic gases. The axes accelerations x, y, z are, respectively, $a_x = Du/Dt$, $a_y = Dv/Dt$ and $a_z = Dw/Dt$. The energy equation is given by the expression:

$$\frac{\partial}{\partial x}\left(k\frac{\partial T}{\partial x}\right)+\frac{\partial}{\partial y}\left(k\frac{\partial T}{\partial y}\right)+\frac{\partial}{\partial z}\left(k\frac{\partial T}{\partial z}\right)+\frac{\partial Q}{\partial t}+$$
$$\Phi_d-\nabla^T\vec{q}_r=\frac{\partial}{\partial x}(\rho u)+\frac{\partial}{\partial y}(\rho v)+\frac{\partial}{\partial z}(\rho w)+ \quad (9)$$
$$\frac{\rho}{2}\frac{D}{Dt}\left(u^2+v^2+w^2\right)+\rho\frac{DE}{Dt}$$

where T is the temperature, k the thermal conductivity, Q the heat source of the volume, Φ_d the dissipation function, $\vec{q}_r$ the heat radiation flux vector and E the internal energy.

The boundary conditions applied to the system can be summarized as follows:

a) Ambient temperature of 295 K (summer), 289 K (winter).
b) Wall, ceiling and floor temperature of 295 K
c) Glasses temperature of 313 K (summer), 289 K (winter).
d) Air inflow 575 m^3/h.
e) Irradiance polynomial curves.
f) Body temperature of 303 K.
g) Number of persons in the meeting room.

For the analysis the mesh is constituted by 60883 elements and 99069 degrees of freedom. Figure 6 represents the finite elements mesh.

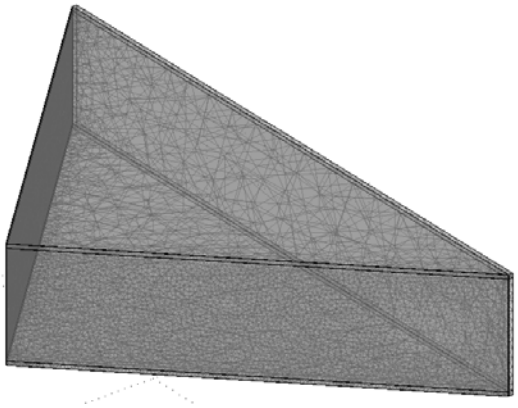

Figure 6 Enclosure's finite elements mesh.

3.1 Experimental validation

The Figure 7 shows a 2D scheme of the meeting room in which are detailed the measure points of temperature. The red points indicate the thermocouple locations used for the experimental evaluation. The Table 4 indicates the reference points coordinates.

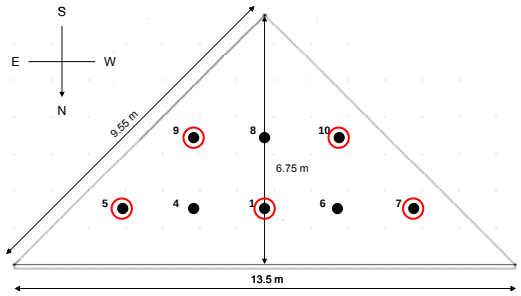

Figure 7 Temperature measurement points. ○, experimental measurement points. ●, reference points.

Figure 8 and Figure 9 compare the evolution of the temperature measured and the provided by the finite elements model. It is observed in both cases a good approximation of the results generated by the numerical model.

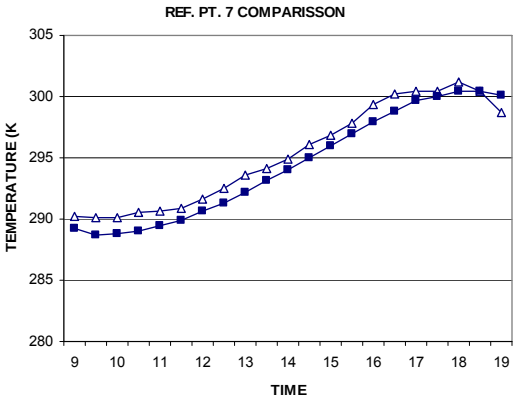

Figure 8 Temperature comparisons at point 7. –Δ–Δ–, experimental measurement; –■–■–, FEM.

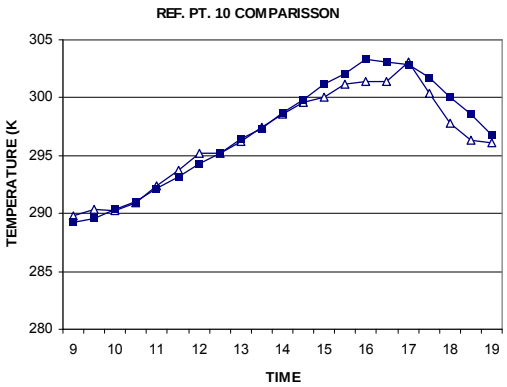

Figure 9 Temperature comparisons at point 10. –Δ–Δ–, experimental measurement; –■–■–, FEM.

3.2 Results

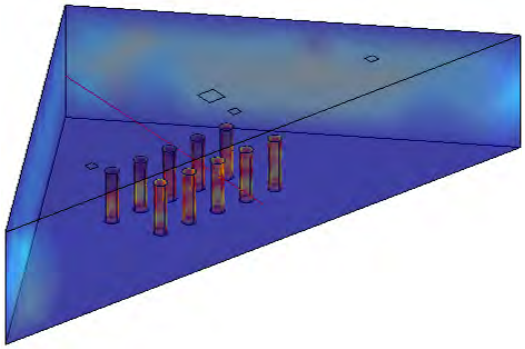

Figure 10 representation of the meeting room with ten people.

The simulations have been carried out taking into account the assumptions described in the scenarios. The results are grouped according to the season, the consideration of air conditioning and the number of people. Figure 10 shows the enclosure with ten people with the most likely position.

3.2.1 Summer

When the air conditioning system is running the results, Figure 11, show a difference when the number of people varies in the enclosure. With ten people the temperature hardly exceeds the upper limit of summer comfort range (296-298) K, established in the RITE [1]. In addition, the temperature is 2 K higher in the case where the room is empty.

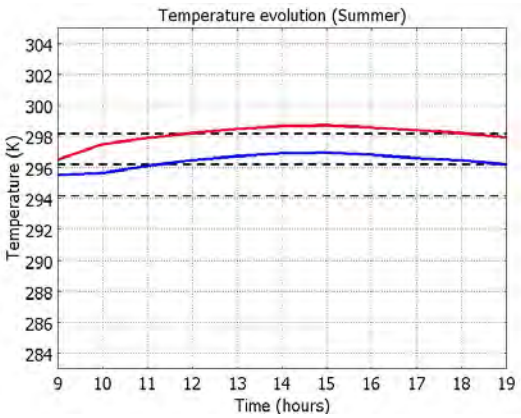

Figure 11 Temperature evolution in summer with air conditioning. ——, 0 people; ——, 10 people.

In contrast when the air conditioning system is off the temperature increases beyond empty room for most of the time the upper limit of comfort. With ten people in it this limit is exceeded by up to 4 K, with obvious results, Figure 12.

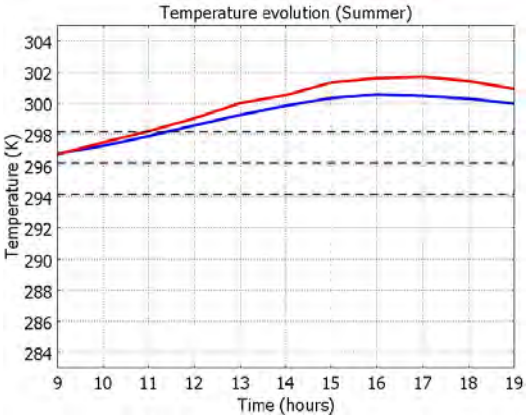

Figure 12 Temperature evolution in summer without air conditioning. ——, 0 people; ——, 10 people.

3.2.2 Winter

In the winter with the air conditioning system running can be seen through Figure 13 a stable performance of the temperature within the comfort ranges for the winter [1] (294-296) K. Room temperature with ten people is slightly higher than with the empty room.

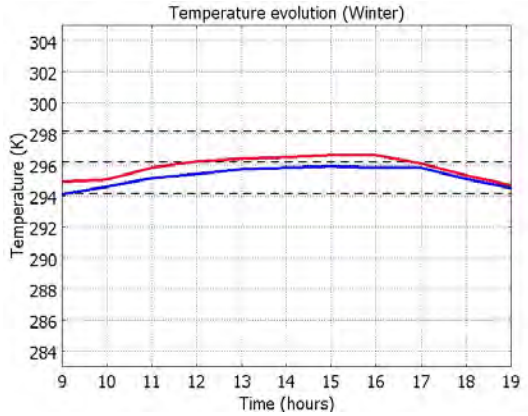

Figure 13 Temperature evolution in winter with air conditioning. ——, 0 people; ——, 10 people.

In the case where the air conditioning system is stopped it appears that in the beginning of the day the temperature is in the range below the threshold of winter comfort range. Throughout the day the temperature of the empty room

develops maintaining it within the comfort range. With ten people temperature is around 298 K, see Figure 14.

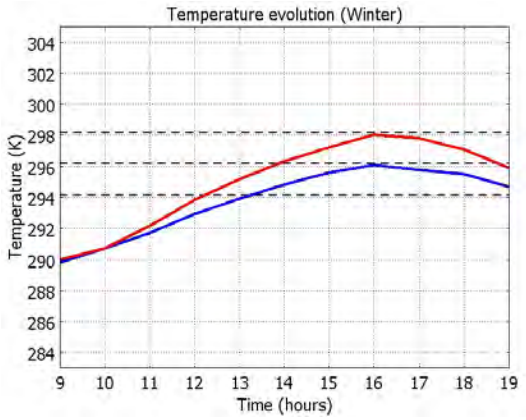

Figure 14 Temperature evolution in winter without air conditioning. ----, 0 people; ----, 10 people.

The comparison of the results shown in Figure 12 and Figure 14 with the one of the Figure 5 and Figure 6 indicates a correlation in the trends of temperature and irradiance. This is a consequence of the geometric characteristics of the enclosure and the materials used in its construction.

4 Conclusions

This work has evaluated the influence of the irradiance in the evolution of the temperature of this enclosure. The polynomial fit of the irradiance curves to the data provided by the weather station have established a good approximation of the temperature trend considering various scenarios. Knowledge of these developments will set the appropriate parameters to the control system design that reduces energy consumption.

The use of numerical techniques such as finite element method, through a modeling tool such as Comsol, has provided results that are closer to the data collected through experimental tests.

5 References

1 R.D. 1027/2007 *Reglamento de las instalaciones térmicas en los edificios (RITE)*. 53 p. Boletín Oficial del Estado 207 del 29-08-2007, Madrid (2007).

2 Astley, R. J. *Finite Elements in solids and structures. An introduction*. 345 p. Chapman & Hall, London (1992).

3 Zienkiewicz, O.C. y Taylor, R.L. *The Finite Element Method. Vol. 1. Basics formulations and linear problems*. 648 p. McGraw-Hill, London (1989).

4 European Comission. *PVGIS Datos de Irradiación Solar*. Comisión europea. http://re.jrc.ec.europa.eu/pvgis/.

5 Corberán S., Royo P. *Colección de ejercicios de transmisión de calor*. 319 p. Universidad Politécnica de Valencia, Valencia (2001).

6 Çengel Y. *Transferencia de calor y masa.* 901 p. McGraw-Hill, México (2007).

6 Acknowledgements

The development of this work has been funded by the European Union through the European Regional Development Fund (ERDF), and the IMPIVA (Institute of the Small and Medium-sized Industry) attached to the Industry, Trade and Innovation Regional Minister of the Valencia Regional Government by call for aid for Technological Institutes in the Research and Development program, supported by the file number IMIDIC/2010/19.

7 Appendix

Table 1 Irradiance values obtained from the meteorological station.

Time	Summer (W/m^2)	Winter (W/m^2)
9	296.27	103.57
10	476.91	338.00
11	657.42	552.43
12	772.75	633.57
13	872.53	686.86
14	905.50	748.71
15	865.06	791.71
16	742.65	515.75
17	665.79	248.00
18	519.86	0.00
19	264.55	0.00

Table 2 Irradiance on both surfaces in summer.

Time zone	Summer East face (W/m^2)	Summer West face (W/m^2)
9 to 10	187.54	108.73
10 to 11	262.30	214.61
11 to 12	340.54	316.87
12 to 13	380.97	391.78
13 to 14	372.57	499.96
14 to 15	316.93	588.58
15 to 16	233.57	631.49
16 to 17	163.38	579.27
17 to 18	166.45	499.34
18 to 19	166.35	353.50
> 19	84.66	179.89

Table 3 Irradiance on both surfaces in winter.

Time zone	Winter East face (W/m^2)	Winter West face (W/m^2)
9 a 10	72.50	31.07
10 a 11	206.18	131.82
11 a 12	303.84	248.59
12 a 13	304.11	329.46
13 a 14	281.61	405.25
14 a 15	239.59	509.13
15 a 16	158.34	633.37
16 a 17	67.05	448.70
17 a 18	0.00	248.00
18 a 19	0.00	0.00
> 19	0.00	0.00

Table 4 Coordinates of reference points.

Point	*x*(m)	*y*(m)	*z*(m)
1	-6.75	1.5	1
2	-6.75	1.5	2
3	-6.75	1.5	2.6
4	-8.75	1.5	1
5	-10.75	1.5	1
6	-4.75	1.5	1
7	-2.75	1.5	1
8	-6.75	4	1
9	-8.75	4	1
10	-4.75	4	1